



Published in final edited form as:

Nat Cell Biol. 2009 October ; 11(10): 1225–1232. doi:10.1038/ncb1966.

The planar cell polarity effector Fuz is essential for targeted membrane trafficking, ciliogenesis, and mouse embryonic development

Ryan S. Gray¹, Philip B. Abitua^{*1}, Bogdan J. Wlodarczyk^{*2}, Heather L. Szabo-Rogers⁴, Otis Blanchard¹, Insuk Lee^{5,**}, Greg S. Weiss^{1,5}, Karen J. Liu⁴, Edward M. Marcotte⁵, John B. Wallingford^{***,1}, and Richard H. Finnell^{***,2,3}

¹ Dept. of Molecular Cell and Developmental Biology, Institute for Cellular and Molecular Biology, University of Texas, Austin, Texas 78712

² Center for Environmental and Genetic Medicine, Institute of Biosciences and Technology, Texas A&M Health Science Center, Houston, Texas 77030

³ The Texas A&M Institute for Genomic Medicine, Houston, Texas 77030

⁴ Dept. of Craniofacial Development, King's College London, London, UK SE1 9RT

⁵ Dept. Chemistry and Biochemistry and Center for Systems and Synthetic Biology, University of Texas, Austin, Texas 78712

Abstract

The planar cell polarity (PCP) signaling pathway is essential for embryonic development because it governs diverse cellular behaviors, and the “core PCP” proteins, such as Dishevelled and Frizzled, have been extensively characterized^{1–4}. By contrast, the “PCP effector” proteins, such as Intu and Fuz, remain largely unstudied^{5, 6}. These proteins are essential for PCP signaling, but they have never been investigated in a mammal and their cell biological activities remain entirely unknown. We report here that Fuz mutant mice display neural tube defects, skeletal dysmorphologies, and Hedgehog signaling defects stemming from disrupted ciliogenesis. Using bioinformatics and imaging of an *in vivo* mucociliary epithelium, we establish a central role for Fuz in membrane trafficking, showing that Fuz is essential for trafficking of cargo to basal bodies and to the apical tips of cilia. Fuz is also essential for exocytosis in secretory cells. Finally, we identify a novel, Rab-related small GTPase as a Fuz interaction partner that is also essential for ciliogenesis and secretion. These results are significant because they provide novel insights into the mechanisms by which developmental regulatory systems like PCP signaling interface with fundamental cellular systems such as the vesicle trafficking machinery.

Users may view, print, copy, and download text and data-mine the content in such documents, for the purposes of academic research, subject always to the full Conditions of use:http://www.nature.com/authors/editorial_policies/license.html#terms

John B. Wallingford, wallingford@mail.utexas.edu, 1 University Station C1000, University of Texas, Austin, TX 78712, Phone: 512-232-2784, Fax: 512-471-3878 and Richard H. Finnell, rfinnell@ibt.tamhsc.edu, Institute of Biosciences and Technology, The Texas A&M Health Science Center, 2121 W. Holcombe Blvd., Houston, TX 77030, Phone: 713-677-7777, Fax: 713-677-7790.

*These authors contributed equally.

***Equally-contributing corresponding authors.

**Current address: Network Biotechnology Laboratory, Yonsei University, 134 Shinchon-dong, Seodaemun-gu, Seoul 120-749, South Korea

PCP signaling is essential for a variety of vertebrate developmental events, including morphogenesis of the neural tube, heart, kidney, and ear. Components of the pathway govern a wide array of polarized cellular behaviors, including cell intercalation and migration, cell division, and ciliogenesis^{1, 2}. In *Drosophila* and *Xenopus*, the “PCP effector” proteins, including Fuz, act together with the “core” components such as Dishevelled (Dvl)^{5, 6}. The PCP effectors have received little attention, being the subject of only a single study in vertebrate animals⁶, whereas the core proteins have been the subject of intense study^{1, 2, 7–9}. Fuz is essential for ciliogenesis in *Xenopus*⁶, but its precise molecular function, like that of all intracellular PCP proteins, remains very poorly understood.

We asked if PCP effectors were essential for mammalian development by obtaining murine ES cells with a gene-trap inserted into the second of eleven exons in Fuz, the mouse orthologue of *Drosophila* Fuzzy and *Xenopus* Fuz. This gene trap is predicted to disrupt the transcription of the Fuz gene. These cells were used to generate mice carrying the inactive Fuz allele. Litters from heterozygous matings produced no viable full-term homozygous mutant pups, as the small litters failed to follow expected genotypic ratios upon analysis. Homozygous fetuses were obtained at E18, and these mice displayed a wide range of developmental defects (Fig. 1 and Supp. Fig. 1).

All homozygous mutant mice displayed severe developmental defects, including craniofacial malformations and incompletely penetrant rostral neural tube closure defects, such as exencephaly and encephaloceles (Fig. 1B, Supp. Fig. 1D, E). Some Fuz mutant mice displayed normal neural tube closure despite having severe craniofacial and ocular defects (Supp. Fig. 1F). However, even mice with mild overt neural tube closure defects displayed severe internal hydrocephalus (Supp. Fig. 1H). Fuz mutant mice consistently displayed polydactyly on all limbs (Fig. 1D), and we observed widespread defects in skeletal development and organogenesis, including malformed sternum, ribs, and long bones, as well as severely hypoplastic lungs and conotruncal defects (Fig. 1C–F, I, J; Supp. Fig. 1I–L). This spectrum of defects reflects the phenotype of mice with defects in ciliogenesis^{10, 11}, and is also reminiscent of the defects in human patients with ciliopathic syndromes such as Bardet-Biedl Syndrome^{12, 13}, Meckel-Gruber syndrome¹⁴ or Jeune’s asphyxiating thoracic dystrophy¹⁵

Collectively, these malformations are consistent with a failure of cilia-mediated Hedgehog signaling in Fuz mutant mice, so we next examined the expression of Hedgehog target genes in the spinal cord^{6, 10}. We found that while *Nkx2.2* and *FoxA2* were robustly expressed in the ventral spinal cord of control mice, these expression domains were almost entirely absent in Fuz mutant mice (Fig. 1K–N). Finally, we found that Fuz mutant mice displayed defects in primary ciliogenesis. Immunostaining for acetylated tubulin revealed that primary cilia in the Fuz mutant mice were significantly shorter than cilia of wild-type mice (Fig. 1G–H). Despite the extremely significant difference in average length, the effect on cilia length was variable, and cilia of nearly normal length were occasionally observed in Fuz mutant mice (Supp. Fig. 1B), consistent with the result of Fuz knockdown in *Xenopus*⁶. Moreover, this finding is consistent with the Fuz mutant mouse embryonic phenotypes; Fuz mutants resemble single BBS mutations or hypomorphic alleles of IFT genes, in which cilia are

present but defective^{10, 11}. By contrast, *Kif3a* null mice lack cilia entirely and display far more severe embryonic phenotypes¹⁶.

In addition to these defects in Hedgehog signaling, *Fuz* mutant mice also displayed defects consistent with a failure of PCP signaling. For example, the homozygous *Fuz* mutant mice displayed a kinked or curly tail (Fig. 1B), a phenotype that is consistently associated with heterozygous mutations in core PCP proteins such as *Dvl* or *Vangl2*^{8, 9}. The homozygous *Fuz* mutant mice also displayed cardiac defects, including single outflow tracts and ventral septal defects (Fig. 1J; Supp. Fig. 1L), similar to those observed in mouse models lacking core PCP genes^{2, 8}. The pattern of congenital malformations in the *Fuz* mutant mice is thus entirely consistent with that found in *Xenopus* embryos following *Fuz* knockdown⁶. *Fuz* morphant *Xenopus* embryos and *Fuz* mutant mice each display comparatively mild PCP defects together with more severe defects in cilia-mediated developmental events.

The evolutionarily conserved role for *Fuz* from frogs to mammals provides us an opportunity to exploit the tremendous wealth of bioinformatics data in mammalian systems to help us elucidate the mechanisms of action for the novel *Fuz* protein. We first queried the human interactome for potential *Fuz*-interacting proteins. We noted that high-throughput yeast two-hybrid screening¹⁷ suggested a weak interaction between human *Fuz* and the protein encoded by human Chromosome 1 Open Reading Frame 89 (*Chr1orf89*). BLAST predicted this gene to encode a small GTPase similar to *REM2* and the vesicle-targeting Rab proteins (Supp. Fig. 2A). Based on this homology, we propose renaming *C1orf89* as *Rem/Rab-Similar GTPase 1*, *RSG1*. Co-immunoprecipitation confirmed that *RSG1* associates with *Fuz* (Supp. Fig. 2B).

To assess the function of *RSG1*, we designed an antisense morpholino-oligonucleotide (MO) to block translation of the protein. Dorsally-targeted injection of this MO resulted in defects in rostral neural tube closure, similar to the defects observed in *Fuz* morphants⁶ and in *Fuz* mutant mice (Supp. Fig. 2D, F). Co-injection of GFP-*RSG1* mRNA suppressed the open neural tube phenotype of *RSG1* morphants in a dose-dependent manner, demonstrating that the effect of the MO was specific (Supp. Fig. 2D, G). To examine the function of *RSG1* during ciliogenesis, we made use of the *Xenopus* embryonic epidermis, which is a highly tractable and easily imaged *in vivo* model for mucociliary epithelial development¹⁸. The MO was targeted specifically to the epidermis by ventral injection, thus circumventing the neural tube phenotype. In these morphants, SEM revealed severe defects in ciliogenesis in the epidermal multi-ciliated cells (Fig. 2A–C). This phenotype was very similar to that of *Fuz* knockdown (Fig. 2D).

RSG1 contains the invariant serine/threonine residue whose mutation to asparagine has been shown in other GTPases to alter the guanine nucleotide binding affinity and to generate a dominant-negative protein (Supp. Fig. 2C yellow/pink residues). We therefore mutated this residue and expressed high levels of *RSG1*^{T65N} in *Xenopus* embryos. Overexpression of *RSG1*^{T65N} resulted in defective ciliogenesis in multi-ciliated cells of the epidermis, while we observed no effect from overexpression of wild-type *RSG1* (Fig. 2E, F). These experiments confirm the results of *RSG1* knockdown and suggest that the GTPase activity of *RSG1* is essential for ciliogenesis.

Finally, we examined RSG1 subcellular localization by expression of low levels of GFP-RSG1, and we observed that it localized strongly to the vicinity of basal bodies in multi-ciliated cells (Fig. 2G). This localization is very likely accurate, since GFP-RSG1 can rescue the phenotype of RSG1 morphants (Supp. Fig. 2D, G). By contrast, the GFP-RSG1^{T65N} localized only very poorly to basal bodies (Fig. 2H). Together, the results of knockdown, expression of the dominant-negative, and localization of the GFP-fusion proteins, suggest a role for the RSG1 GTPase in ciliogenesis. These results are consistent with a role for this protein in mediating Fuz function.

Our bioinformatic approach successfully revealed novel aspects of the molecular network in which Fuz functions, so we extended this approach to investigate the cell biological function of the novel protein encoded by the Fuz gene. We turned to mouseFUNC, a large-scale community effort to systematically predict mouse gene function using the consensus of diverse computational approaches¹⁹. MouseFUNC predicted a central role in vesicle trafficking for Fuz (Supp. Fig. 3A). This suggestion was supported by results of iterative BLAST searches (PSIBLAST), which identified modest similarity between Fuz and the yeast vacuolar fusion protein Mon1 (data not shown).

We next used homology modeling^{20, 21} to predict the structure of the Fuz protein. Using mGENTHREADER (see Supplemental Methods), we predicted that the C-terminus of the *Xenopus* Fuz protein should fold into a series of five β -sheets flanked by α -helices (Fig. 3A, B; Supp. Fig. 3C, D). This structure, known as a longin-domain²², is consistent with a vesicle trafficking function for Fuz. Indeed, the longin-domain is present in the structure of SEDL, a subunit of the vesicle-tethering TRAPP complex that is associated with skeletal dysmorphogenesis^{23, 24}. Moreover, the longin-domain is shared by several other vesicle trafficking proteins, including subunits of the AP clathrin adaptor complexes²⁵ and the membrane-fusing SNARE proteins, sec22b, VAMP7, and Ytk6p (Refs. 22, 26).

These longin-domain containing proteins are all tightly linked to one another in probabilistic networks of human, mouse, and yeast genes, and this node within the gene networks is tightly linked to other core vesicle-trafficking proteins (Supp. Fig. 4; and see Supplemental Methods). However, the scale of these linkages was too large to generate easily testable hypotheses. We therefore returned to the physical interactome data, looking this time for relationships between longin-domain containing proteins with structural similarity to the Fuz C-terminus. We found that the longin-domain proteins AP2 σ , AP1 σ , and SEDL were all linked by physical associations to the PCP protein Dvl2 (Fig. 3C), which interacts genetically with Fuz^{5, 6}. More importantly, AP2 σ , AP1 σ , SEDL and Dvl2 were all linked by physical association to the CaLponin Homology and Microtubule-associated Protein (CLAMP, also called spf1; Fig. 3C), a microtubule-bundling protein that is a known component of cilia and flagella^{7, 27,28}.

Since Fuz is essential for ciliogenesis, we asked if Fuz may play a role in CLAMP localization. In living *Xenopus* embryos, CLAMP-GFP labeled the axonemes of cilia in multi-ciliated cells (Fig. 3D, left), as has been reported previously for sperm flagella²⁸. In addition to the axonemal labeling, however, we also observed an obvious enrichment at the apical tips of cilia (Fig. 3D, left). To test the effect of Fuz knockdown, we used targeted

injection to generate *in vivo* mosaic epidermis, where control and morphant cells are intermingled. In these mosaics, the morphant cells are indicated specifically by co-injected mRNA encoding histone 2B-RFP (nucRFP; Fig. 3D, inset). In nucRFP-positive Fuz morphant cells, CLAMP-GFP was visible in the shortened and dysmorphic cilia, but the normal accumulation of CLAMP-GFP at the apical tips was entirely absent (Fig. 3D, right).

This role for Fuz in CLAMP localization was of particular interest because we previously found that CLAMP also co-localizes with Dvl2 in the vicinity of the ciliary rootlet⁷, which is a known nexus for vesicle trafficking to cilia^{7, 29, 30}. In control embryos, CLAMP-GFP is restricted to the apical cell surface, where it formed a well-defined, linear structure adjacent to the apically-docked basal bodies indicated by co-expressed centrin-RFP (Fig. 4A, a', a'' and see Refs. 7, 18). In contrast to controls, the CLAMP-GFP signal in Fuz morphant embryos was present in larger, irregularly-shaped foci. Z-projections revealed that many of these irregular foci were well below the apical cell surface (Fig. 4B, b', b''), though centrin-RFP formed an even line at the apical surface of these cells. This result indicates that Fuz, unlike Dvl (Ref. 6), is not essential for apical docking of basal bodies, but is essential for apical trafficking of CLAMP. The dual localization of CLAMP-GFP at the basal apparatus and at the apical tip is reminiscent of IFT88 and IFT52 in mammalian cells³¹, and our data suggest that Fuz is required for accumulation of CLAMP at both sites.

Because the RSG1 GTPase binds to Fuz and is essential for ciliogenesis, we predicted interference with RSG1 function would elicit a similar CLAMP trafficking phenotype. Indeed, in mosaic embryos, nucRFP-positive RSG1 morphant cells displayed defects in the trafficking of CLAMP-GFP to the apical cell surface, while nearby control cells displayed no such defects (Fig. 4C, D). In addition, expression of RSG1^{T65N} also severely disrupted apical trafficking of CLAMP-GFP, while expression of wild-type RSG1 had little effect (Supp. Fig. 5). Finally, RSG1 knockdown also eliminated the accumulation of CLAMP-GFP to the apical tips of cilia in multi-ciliated cells (Fig. 4E).

Our data thus demonstrate that Fuz and RSG1 act to regulate trafficking during ciliogenesis. Because longin-domain proteins participate in many fundamental vesicle trafficking events²², we next asked if Fuz might play a broader role in trafficking than is reflected by the phenotype in multi-ciliated cells. We examined the mucus-secreting goblet cells that surround the multi-ciliated cells in the *Xenopus* epidermis¹⁸. Scanning electron microscopy (SEM) demonstrated that the apical surface of the goblet cells in controls were decorated with numerous open exocytic vesicles, many of which were actively releasing mucus granules (Fig. 5A). By contrast, open exocytic vesicles were extremely rare and few mucus granules were visible on goblet cells in Fuz morphants (Fig. 5B). We also observed that either knockdown of RSG1 or overexpression of RSG1^{T65N} elicited defects in exocytosis in mucus-secreting cells (Fig. 2C, F), suggesting that this GTPase is a key effector of Fuz function in multiple cell types.

To confirm the failure of secretion in Fuz morphant goblet cells, we turned again to mosaic epidermis where we examined immunostaining for Intelectin2, a major component of the secreted *Xenopus* epidermal mucus^{18, 32}. In control cells of these mosaics (indicated by an absence of membrane-RFP co-injected with the MO), Intelectin2 in exocytosing mucus

granules was visible as discrete foci, at or above the apical surface (Fig. 5D, d'). By contrast, Intelectin2 signal was present only below the apical cell surface in neighboring morphant cells (indicated by the presence of co-injected membrane-RFP in Fig. 5D, d'). The failure of exocytosis in morphant cells in these mosaic epithelia was also confirmed by SEM (Fig. 5C).

The joining of membrane compartments proceeds through discrete steps of transport, tethering, and fusion³³. Our bioinformatic analyses suggested a possible relationship between Fuz and either vesicle tethering or membrane fusion processes (Supp. Fig. 4), and electron microscopy of Fuz morphants supports the latter relationship. TEM revealed that morphant goblet cells often were decorated by large apical membrane blebs atop putative exocytic vesicles (Fig. 5F, green arrowhead) and this phenotype was obvious in SEM (Fig. 5B, green arrowheads). Such apical membrane blebs were also apparent in RSG1 morphants (Fig. 2B, C). Many mucus-filled vesicles in Fuz morphants appeared to be tethered to the apical plasma membrane, though very few had fused (Fig. 5F).

The finding that mucus-filled vesicles in Fuz morphant cells tether to, but fail to fuse with, the apical plasma membrane might suggest a general role for Fuz in governing vesicle fusion. However, secretion in *Xenopus* goblet cells can proceed by compound exocytosis, in which secretory vesicles fuse with one another as they approach the plasma membrane^{3, 34–36}. We also observed such homotypic fusion of mucus-containing vesicles in Fuz morphants, despite the failure of nearby, apparently tethered, vesicles to fuse with the plasma membrane (Fig. 5F, red arrow; Supp. Fig. 6B, C). In some cases, vesicles were observed that had fused to one another, but had not yet tethered to the apical plasma membrane (Supp. Fig. 6B, arrows). These data demonstrate that Fuz is essential for mediating only a specific subset of membrane fusion events.

The PCP signaling cascade is broadly required for development of vertebrate embryos. However, studies to date have focused on only a small number of the known PCP genes, such as Dvl and Vangl2 (Refs. 2, 7–9). Here, we have demonstrated that the largely unstudied PCP effector protein Fuz is fundamentally necessary for embryonic development in vertebrates. Our data suggest a central role for Fuz in regulating targeted membrane fusion events, and this cellular function can explain the phenotype of embryos lacking Fuz function.

First, vesicle trafficking to the basal body and within axonemes is essential for ciliogenesis (e.g. Refs. 7, 29–31), and the phenotypes observed in *Xenopus* or mouse embryos lacking Fuz function reflect those observed in mice lacking key ciliogenesis factors, such as the BBS or IFT proteins^{10, 11}. A key role of the cilium in development is thought to be the transduction of Hedgehog signaling¹⁰, so it is relevant that Hedgehog target gene expression is lost in Fuz morphant *Xenopus* embryos⁶ and in Fuz mutant mice (Fig. 1). Secondly, defective secretion in cells lacking Fuz function may also contribute to the embryonic phenotype. We observed severe skeletal defects in vertebrate embryos lacking Fuz function (Fig. 1 and Ref 6); skeletal defects are likewise observed in humans or zebrafish with mutations in Sec23A, a subunit of the COPII complex^{37, 38} and in humans with mutations in the TRAPP complex subunit, SEDL (Ref. 24).

Our data therefore place Fuz and the interacting GTPase RSG1 at the interface of developmental regulatory systems (e.g. PCP signaling) and fundamental cell biological processes (e.g. ciliogenesis, secretion). In combination with the finding that Dvl mediates vesicle association with basal bodies in ciliated cells⁷, the data here suggest that coordination of vesicle trafficking may be a unifying mechanism by which PCP signaling can control so many diverse cellular behaviors during embryonic development.

Materials and Methods

The Materials and Methods used in this work are described in the Supplemental Information.

Supplementary Material

Refer to Web version on PubMed Central for supplementary material.

Acknowledgments

The ES cell clone for making the Fuz mutant mouse was generously provided by Lexicon Pharmaceuticals. We thank P. Paukstelis for aid with structural modeling, S. Vokes for critical comments on the manuscript, and Wei H. for technical help with histology and immunostaining. Phil Abitua is supported by a Diversity Supplement from the NIH/NIGMS. This work was supported by grants to K.J.L. from the Wellcome Trust and the BBSRC; to E.M.M. from the NSF, NIH, Welch Foundation (F-1515), Texas Institute for Drug and Diagnostic Development, and a Packard Fellowship; grants to J.B.W. from the NIH/NIGMS, The March of Dimes, The Burroughs Wellcome Fund, the Sandler Program for Asthma Research, and the Texas Advanced Research Program; and by grants to R.H.F. from the NIH and The Texas A&M Institute for Genomic Medicine.

References

1. Wallingford JB. Planar cell polarity, ciliogenesis and neural tube defects. *Hum Mol Genet.* 2006; 15(Spec No 2):R227–234. [PubMed: 16987888]
2. Karner C, Wharton KA Jr, Carroll TJ. Planar cell polarity and vertebrate organogenesis. *Semin Cell Dev Biol.* 2006; 17:194–203. [PubMed: 16839790]
3. Simons M, Mlodzik M. Planar cell polarity signaling: from fly development to human disease. *Annu Rev Genet.* 2008; 42:517–540. [PubMed: 18710302]
4. Collier S, Gubb D. Drosophila tissue polarity requires the cell-autonomous activity of the fuzzy gene, which encodes a novel transmembrane protein. *Development.* 1997; 124:4029–4037. [PubMed: 9374400]
5. Lee H, Adler PN. The function of the frizzled pathway in the Drosophila wing is dependent on inturned and fuzzy. *Genetics.* 2002; 160:1535–1547. [PubMed: 11973308]
6. Park TJ, Haigo SL, Wallingford JB. Ciliogenesis defects in embryos lacking inturned or fuzzy function are associated with failure of planar cell polarity and Hedgehog signaling. *Nat Genet.* 2006; 38:303–311. [PubMed: 16493421]
7. Park TJ, Mitchell BJ, Abitua PB, Kintner C, Wallingford JB. Dishevelled controls apical docking and planar polarization of basal bodies in ciliated epithelial cells. *Nat Genet.* 2008; 40:871–879. [PubMed: 18552847]
8. Hamblet NS, et al. Dishevelled 2 is essential for cardiac outflow tract development, somite segmentation and neural tube closure. *Development.* 2002; 129:5827–5838. [PubMed: 12421720]
9. Kibar Z, et al. Ltap, a mammalian homolog of Drosophila Strabismus/Van Gogh, is altered in the mouse neural tube mutant Loop-tail. *Nat Genet.* 2001; 28:251–255. [PubMed: 11431695]
10. Huangfu D, et al. Hedgehog signalling in the mouse requires intraflagellar transport proteins. *Nature.* 2003; 426:83–87. [PubMed: 14603322]

11. Ross AJ, et al. Disruption of Bardet-Biedl syndrome ciliary proteins perturbs planar cell polarity in vertebrates. *Nat Genet.* 2005; 37:1135–1140. [PubMed: 16170314]
12. Ansley SJ, et al. Basal body dysfunction is a likely cause of pleiotropic Bardet-Biedl syndrome. *Nature.* 2003; 425:628–633. [PubMed: 14520415]
13. Sharma N, Berbari NF, Yoder BK. Ciliary dysfunction in developmental abnormalities and diseases. *Curr Top Dev Biol.* 2008; 85:371–427. [PubMed: 19147012]
14. Smith UM, et al. The transmembrane protein meckelin (MKS3) is mutated in Meckel-Gruber syndrome and the wpk rat. *Nat Genet.* 2006; 38:191–196. [PubMed: 16415887]
15. Beales PL, et al. IFT80, which encodes a conserved intraflagellar transport protein, is mutated in Jeune asphyxiating thoracic dystrophy. *Nat Genet.* 2007; 39:727–729. [PubMed: 17468754]
16. Takeda S, et al. Left-right asymmetry and kinesin superfamily protein KIF3A: new insights in determination of laterality and mesoderm induction by kif3A^{-/-} mice analysis. *J Cell Biol.* 1999; 145:825–836. [PubMed: 10330409]
17. Rual JF, et al. Towards a proteome-scale map of the human protein-protein interaction network. *Nature.* 2005; 437:1173–1178. [PubMed: 16189514]
18. Hayes JM, et al. Identification of novel ciliogenesis factors using a new in vivo model for mucociliary epithelial development. *Dev Biol.* 2007; 312:115–130. [PubMed: 17961536]
19. Pena-Castillo L, et al. A critical assessment of *Mus musculus* gene function prediction using integrated genomic evidence. *Genome Biol.* 2008; 9 (Suppl 1):S2. [PubMed: 18613946]
20. Ginalski K. Comparative modeling for protein structure prediction. *Curr Opin Struct Biol.* 2006; 16:172–177. [PubMed: 16510277]
21. Hagiwara H, Aoki T, Ohwada N, Fujimoto T. Development of striated rootlets during ciliogenesis in the human oviduct epithelium. *Cell Tissue Res.* 1997; 290:39–42. [PubMed: 9377640]
22. Rossi V, et al. Longins and their longin domains: regulated SNAREs and multifunctional SNARE regulators. *Trends Biochem Sci.* 2004; 29:682–688. [PubMed: 15544955]
23. Jang SB, et al. Crystal structure of SEDL and its implications for a genetic disease spondyloepiphyseal dysplasia tarda. *J Biol Chem.* 2002; 277:49863–49869. [PubMed: 12361953]
24. Gedeon AK, et al. Identification of the gene (SEDL) causing X-linked spondyloepiphyseal dysplasia tarda. *Nat Genet.* 1999; 22:400–404. [PubMed: 10431248]
25. Collins BM, McCoy AJ, Kent HM, Evans PR, Owen DJ. Molecular architecture and functional model of the endocytic AP2 complex. *Cell.* 2002; 109:523–535. [PubMed: 12086608]
26. Pryor PR, et al. Molecular basis for the sorting of the SNARE VAMP7 into endocytic clathrin-coated vesicles by the ArfGAP Hrb. *Cell.* 2008; 134:817–827. [PubMed: 18775314]
27. Dougherty GW, et al. CLAMP, a novel microtubule-associated protein with EB-type calponin homology. *Cell Motil Cytoskeleton.* 2005; 62:141–156. [PubMed: 16206169]
28. Chan SW, Fowler KJ, Choo KH, Kalitsis P. Spef1, a conserved novel testis protein found in mouse sperm flagella. *Gene.* 2005; 353:189–199. [PubMed: 15979255]
29. Fariss RN, Molday RS, Fisher SK, Matsumoto B. Evidence from normal and degenerating photoreceptors that two outer segment integral membrane proteins have separate transport pathways. *J Comp Neurol.* 1997; 387:148–156. [PubMed: 9331178]
30. Yang J, Li T. The ciliary rootlet interacts with kinesin light chains and may provide a scaffold for kinesin-I vesicular cargos. *Exp Cell Res.* 2005; 309:379–389. [PubMed: 16018997]
31. Follit JA, Tuft RA, Fogarty KE, Pazour GJ. The intraflagellar transport protein IFT20 is associated with the Golgi complex and is required for cilia assembly. *Mol Biol Cell.* 2006; 17:3781–3792. [PubMed: 16775004]
32. Nagata S, Nakanishi M, Nanba R, Fujita N. Developmental expression of XEEL, a novel molecule of the *Xenopus* oocyte cortical granule lectin family. *Dev Genes Evol.* 2003; 213:368–370. [PubMed: 12802587]
33. Cai H, Reinisch K, Ferro-Novick S. Coats, tethers, Rabs, and SNAREs work together to mediate the intracellular destination of a transport vesicle. *Dev Cell.* 2007; 12:671–682. [PubMed: 17488620]
34. Billett FS, Gould RP. Fine structural changes in the differentiating epidermis of *Xenopus laevis* embryos. *J Anat.* 1971; 108:465–480. [PubMed: 5575314]

35. Nachury MV, et al. A core complex of BBS proteins cooperates with the GTPase Rab8 to promote ciliary membrane biogenesis. *Cell*. 2007; 129:1201–1213. [PubMed: 17574030]
36. Sorokin SP. Reconstructions of centriole formation and ciliogenesis in mammalian lungs. *J Cell Sci*. 1968; 3:207–230. [PubMed: 5661997]
37. Boyadjiev SA, et al. Cranio-lenticulo-sutural dysplasia is caused by a SEC23A mutation leading to abnormal endoplasmic-reticulum-to-Golgi trafficking. *Nat Genet*. 2006; 38:1192–1197. [PubMed: 16980979]
38. Lang MR, Lapierre LA, Frotscher M, Goldenring JR, Knapik EW. Secretory COPII coat component Sec23a is essential for craniofacial chondrocyte maturation. *Nat Genet*. 2006; 38:1198–1203. [PubMed: 16980978]

Author Manuscript

Author Manuscript

Author Manuscript

Author Manuscript

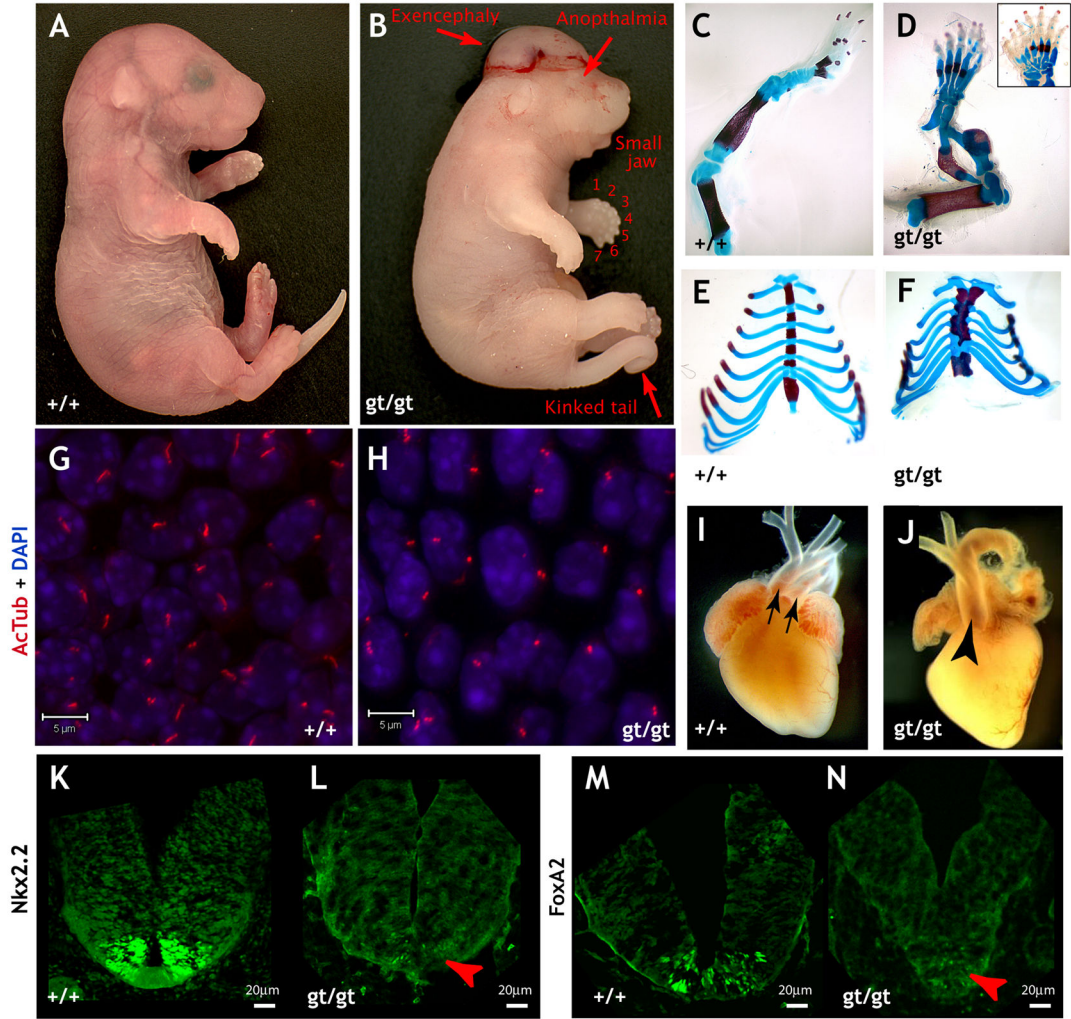


Figure 1. Mice lacking a functional *Fuz* gene display multiple developmental defects. **(a)** Control mouse, E18.5 and **(b)** *Fuz^{gt/gt}* mouse. Skeletal preparation of **(c)** control hindlimb and **(d)** *Fuz^{gt/gt}* hindlimb. Inset shows a paw with extreme polydactyly from a *Fuz^{gt/gt}* mouse. **(e, f)** Sternum preparations from control and *Fuz^{gt/gt}* mouse. **(g, h)** Confocal projections of Meckel's cartilage stained with acetylated tubulin (red) and DAPI (blue) exhibits diminished primary cilia in *Fuz^{gt/gt}* mouse sections. Scale bars = 5µm. Mean cilia length +/- SEM = 1.73 +/- 0.06µm in WT (n=70) and 0.87 +/- 0.04µm in *Fuz^{gt/gt}* (n=52); p<0.001. **(i)** Dissected heart from a control mouse, arrows indicate outflow tracts. **(j)** Dissected heart from a *Fuz^{gt/gt}* mouse, arrowhead indicates single outflow tract. **(k, l)** Expression of *Nkx2.2* (green) in the ventral neural tube is diminished in *Fuz^{gt/gt}* mice (red arrowhead). **(m, n)** Expression of *FoxA2* (green) in the ventral neural tube is lost in *Fuz^{gt/gt}* mice (red arrowhead).

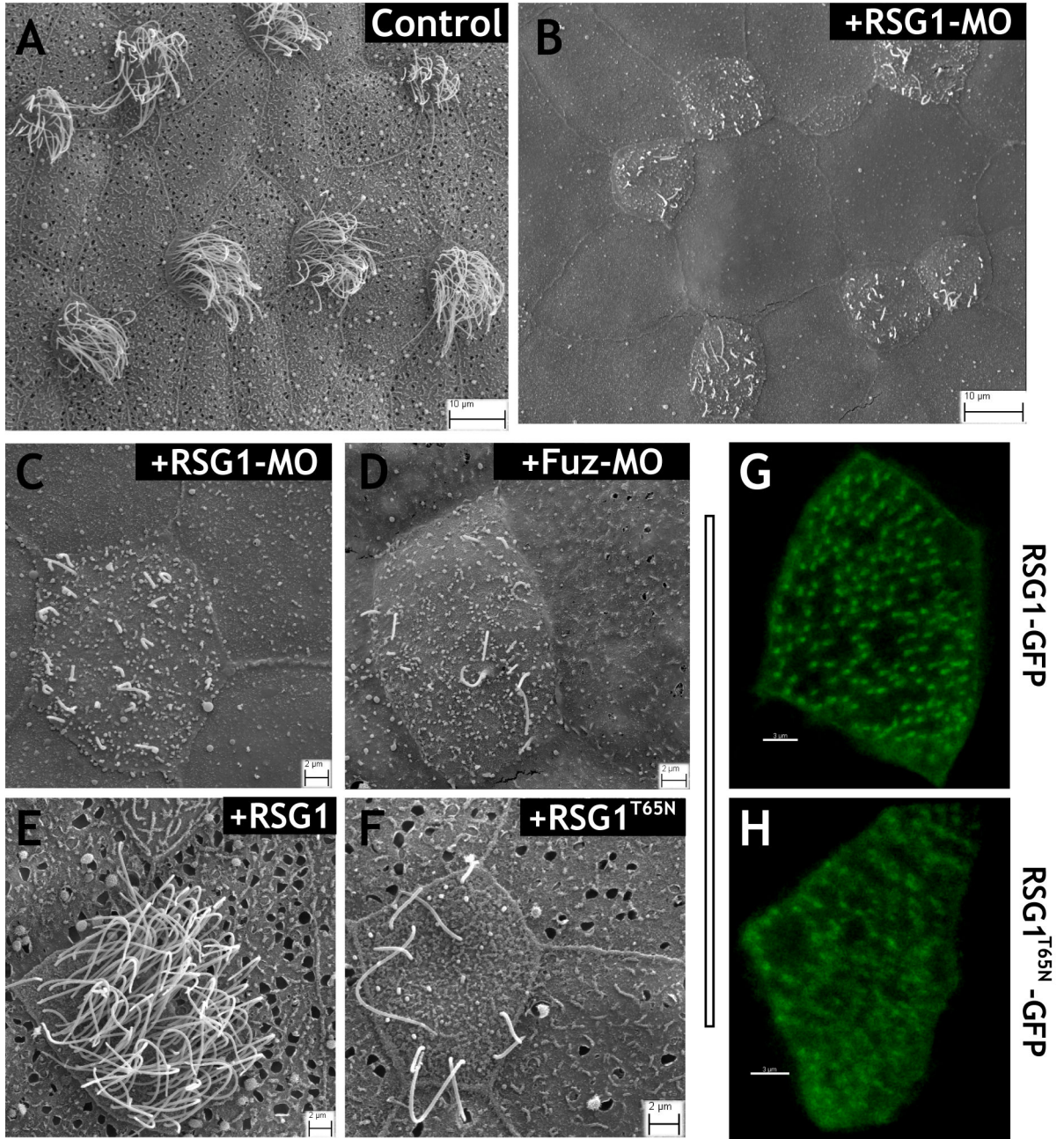


Figure 2. RSG1 controls ciliogenesis and secretion. **(a)** SEM of intact, control *Xenopus* ciliated epidermis reveals multi-ciliated cells and surrounding mucous secreting cells **(b)** RSG1 morphants display defects in ciliogenesis and absence of mucous granules and exocytic pits. **(c)** Higher-magnification view of RSG1 morphant ciliated epidermis displaying diminished cilia numbers and lengths and a decrease in exocytic pits in neighboring secretory cells. **(d)** Fuz morphants also display diminished cilia numbers and lengths and a decrease in exocytic pits in secretory cells. **(e, f)** Epidermal targeted over-expression of RSG1^{T65N}, but not wild type RSG1, results in defects in ciliogenesis as well as decreases in mucous granules and

exocytic pits in secretory cells. **(g, h)** GFP-RSG1 (low-level expression) localizes to the basal body region of multi-ciliated cells, whereas GFP-RSG1^{T65N} (low-level expression) in multi-ciliated cells is diffuse and not tightly associated with basal bodies. Observations of fluorescence levels following expression of GFP-RSG1 and GFP-RSG1^{T65N} mRNA were comparable, suggesting similar rates of translation for the two proteins.

Author Manuscript

Author Manuscript

Author Manuscript

Author Manuscript

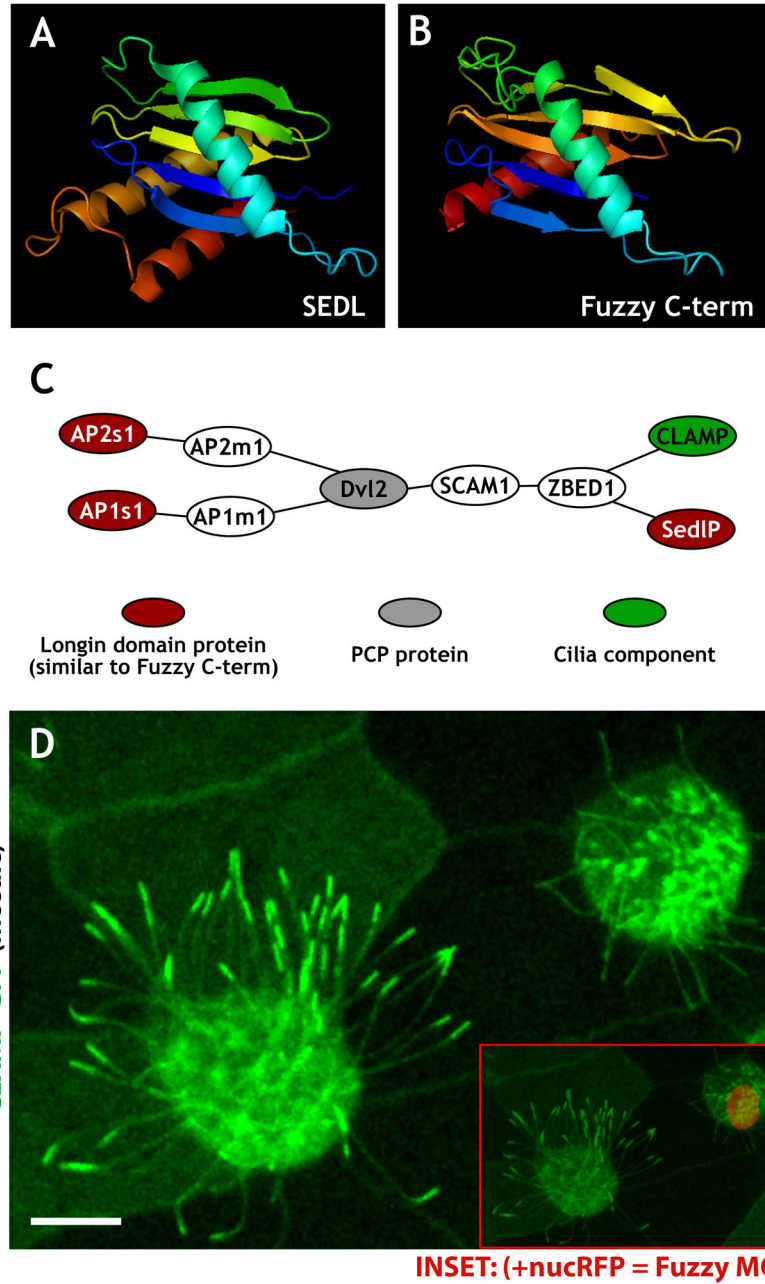


Figure 3. Homology modeling, network predictions, and experimental validation suggest a trafficking function for Fuz. **(a, b)** Rendered protein models (Open-Source PyMOL 0.99rc6 software). **(a)** Sedl N-terminal domain (pdb:1H3Q). **(b)** 1H3Q based homology threaded model of the C-terminal -aa(s) 287–419 - of *Xenopus* Fuz protein. **(c)** Illustration of experimentally-derived protein-protein interactions (see Supplemental Methods) linking Dvl2 with longin-domain proteins AP1s, AP2s, and SedIP as well as CLAMP. **(d)** Mosaic imaging of live embryo expressing CLAMP-GFP, which localizes to ciliary axonemes and apical tips. A nucRFP marks the nuclei, serving as a lineage tracer for co-injected Fuz MO. The confocal

slice reveals a loss of apical localized CLAMP-GFP at ciliary tips in FUZMO cells (inset shows merge of (e) and a more basal slice to display nucRFP signal). Scale bar in (e) = 10uM.

Author Manuscript

Author Manuscript

Author Manuscript

Author Manuscript

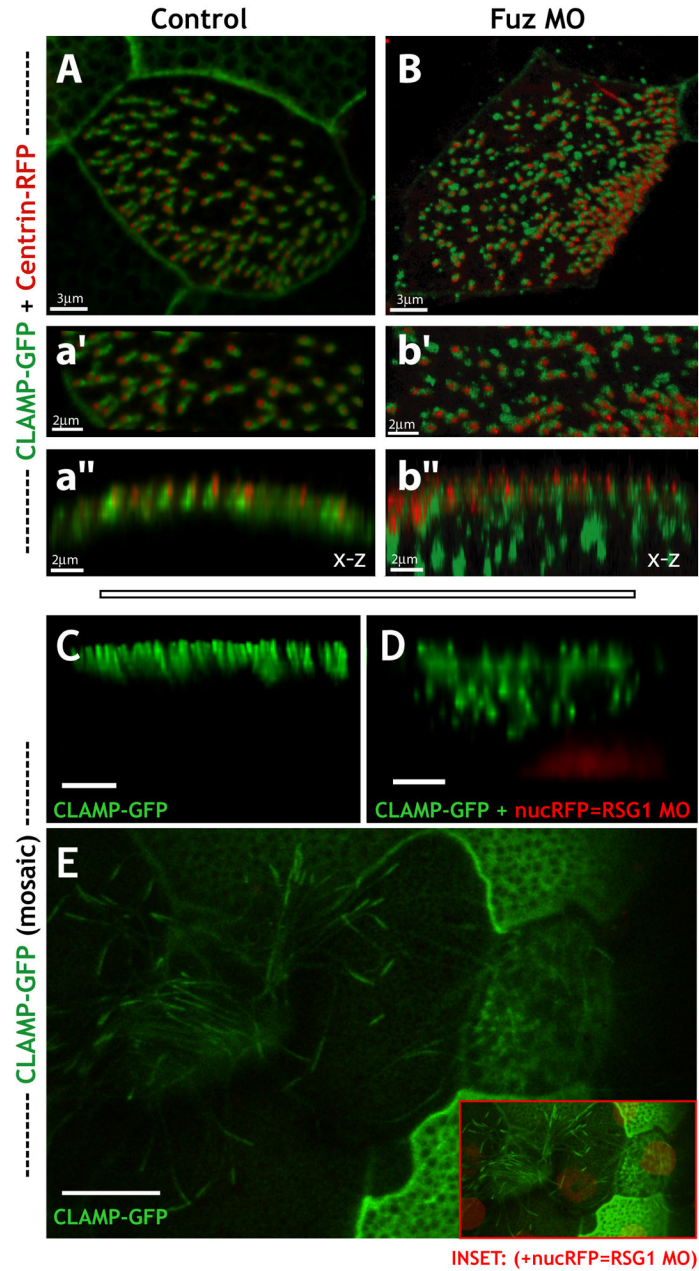


Figure 4.

Fuzzy and RSG1 control trafficking to basal bodies as well as to the tips of cilia. **(a, b)** Fuz knockdown disrupts localization of CLAMP-GFP to the ciliary rootlet. Confocal stacks of formaldehyde fixed *Xenopus* epidermis expressing centrin-RFP and CLAMP-GFP mRNAs. **(a)** Multi-ciliated cell in x-y view from an uninjected control embryo exhibits elongated CLAMP-GFP signal extending from relatively evenly spaced basal bodies (centrin-RFP). **(a')** Higher magnification view of the x-y section from **[a]**. **(a'')** X-Z projection of the stack shown in **[a']** displays apical co-localization of centrin-RFP and CLAMP-GFP. **(b)** Ciliated cell in an x-y view of the apical surface in a Fuz morphant reveals defects in the spacing of centrin-RFP signal and defects in elongated CLAMP-GFP signal. Additionally CLAMP-

GFP signal is not faithfully co-localized with centrin-RFP signal in many cases. **(b')** Higher magnification view of the x-y section from **[b]**. **(b'')** X-Z-projection of the stack shown in **[b]** reveals apical alignment of the centrin-RFP signal however in many cases the CLAMP-GFP signal is below the apical surface in large punctae. **(c-e)** Mosaic imaging of live agarose embedded embryo. CLAMP-GFP highlights a variety of epidermal structures. RFP-Histone 2B (nuc-RFP) serves as a lineage tracer for morpholino-injected cells. **(c, d)** 3D projections (x-z). RSG1 MO (+ nucRFP cells) display defects in normal CLAMP-GFP localization along the apical surface. **(e)** Confocal slice (x-y) exhibiting a loss of apical localized CLAMP-GFP to ciliary tips in RSG1 MO cells (inset shows merge of **(e)** and more basal slice to display nucRFP signal). Scale bars in **(c, d)** are 3 μ M; scale bar in **(e)** is 10 μ m.

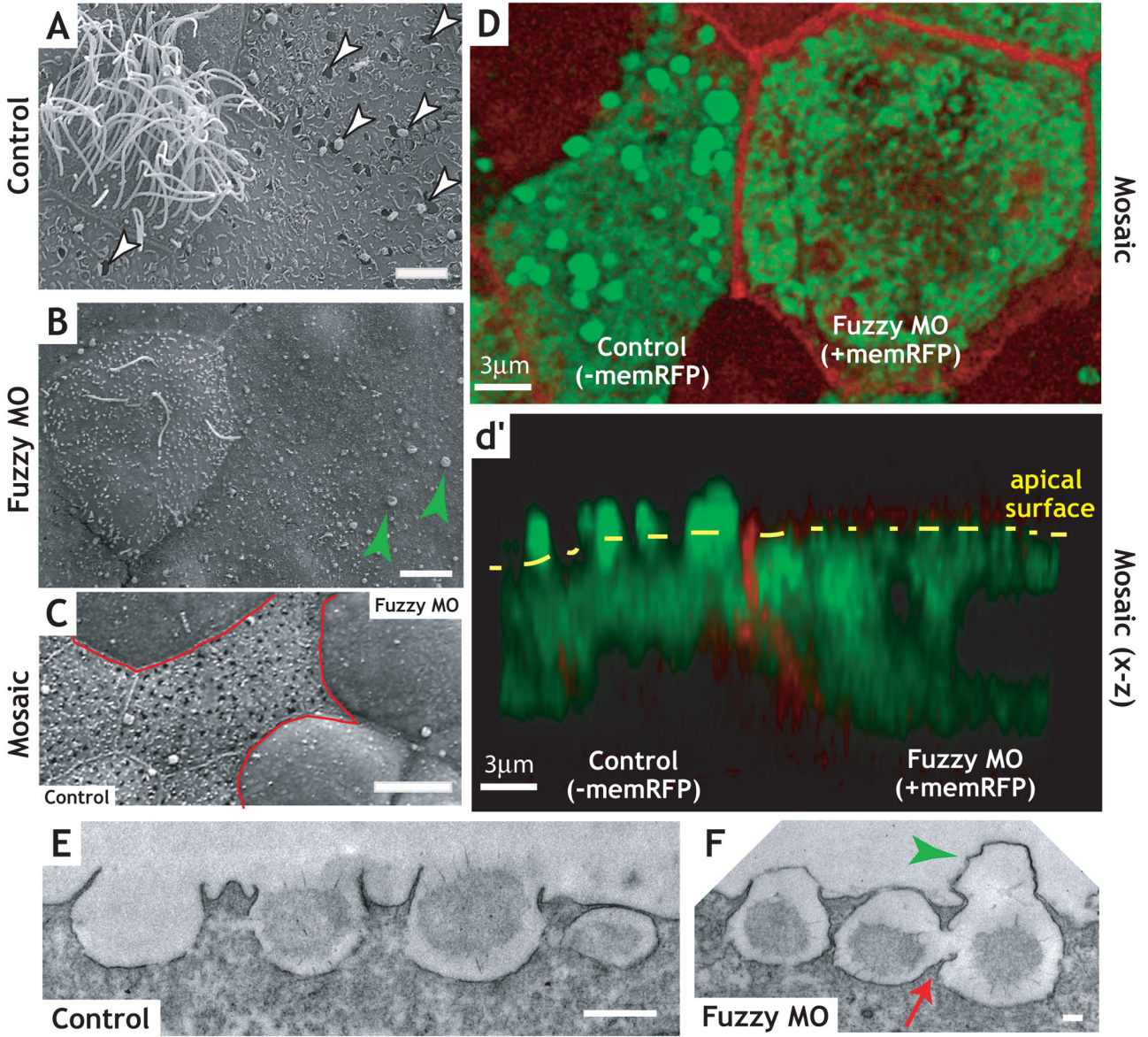


Figure 5. Knockdown of Fuz disrupts exocytosis in mucus-secreting cells. **(a)** Wild type multi-ciliated cell (left) flanked by secretory cells in *Xenopus* mucociliary epidermis. Control cells have an average of over 90 open exocytic pits per cell. **(b)** Fuz morphants display defects in ciliogenesis in multi-ciliated cell (left) and failure of exocytosis in mucus-secreting cells (note the absence of exocytic pits indicated by white arrowheads in **[a]**). Green arrowheads indicate apical membrane blebs (see also panel F, below). In a representative experiment, Fuz morphant cells had fewer than 5 exocytic pits per cell on average (difference from control is significant by the Mann-Whitney U-test; $p < 0.0001$). Scale bars in A, B = 5 μ m **(c)** Mosaic epidermal tissue, with morphant cells outlined in red. Scale bar = 10 μ m **(d)** Confocal section (x-y) of mosaic embryo in which membrane-RFP (memRFP, red) mRNA was co-injected with Fuz morpholino and processed for Xeel (interlectin-2) antibody (green). Cell

expressing a high level memRFP (right) lacks apical Xeel antibody staining comparable to the neighboring cell (right). (**d'**) Confocal projection (x-z) of [**d**] illustrates the loss of apical Xeel staining (green) in the Fuz morphant cell correlated with apical memRFP expression (right). Scale bars in D, d' = 3 μ m (**e**) TEM of section of control *Xenopus* epidermis shows empty and mucus granule-containing vesicles docked at the apical surface, whereas Fuz morphants (**f**) display a defect of vesicle fusion with the plasma membrane release, as illustrated by large membrane protrusions (green arrows in [**b**, **f**]). Additionally, frequent homotypic vesicle fusion events were observed in secretory cells of Fuz morphants (red arrow). Scale bar in E = 500nm; Scale bar in F= 100nm.